

MBE Growth and Characterization of InAsSb Films on GaAs (001) Substrate

Zifan Huo^{1,2}, Yanhui Zhang², and Zezhong Chen^{1,*}

¹ School of Materials and Chemistry, University of Shanghai for Science and Technology, Shanghai 200093, China

² State Key Laboratories of Infrared Physics, Shanghai Institute of Technical Physics, Chinese Academy of Sciences, Shanghai 200083, China

*543553073@qq.com

Abstract

InAsSb films with different As composition were prepared on GaAs (001) substrates by molecular beam epitaxy (MBE) method. The InAs_xSb_{1-x} films were characterized by the High-resolution X-ray diffraction (HRXRD), atomic force microscope (AFM), Fourier transform infrared (FTIR) transmission spectra and Raman spectra. The results indicate that the absorption edge of our InAs_{0.4}Sb_{0.6} sample can achieve 0.1eV at room temperature. The influence of As composition on the surface morphology and absorption edge of our middle as InAs_{0.4}Sb_{0.6} sample can achieve 0.1eV at room temperature. The influence of As composition on the surface morphology and absorption edge of the InAsSb were studied in detail. The Raman spectra of the InAsSb films exhibit two-mode behavior. With the increasing of the As composition of InAsSb, the red shift of the InSb-like LO peaks and blue shift linearly of the InAs-like LO peaks were observed.

Keywords

InAsSb; MBE; GaAs (001); HRXRD; AFM; FTIR.

1. Introduction

InAsSb ternary alloy has got great attentions for the potential application to high-speed electronic and opto-electronic device in the wavelength range of 3-5 μ m and 8-12 μ m windows where the atmospheric absorption is minimum[1-5]. In recent years, InAsSb infrared detectors with high operating temperatures (HOT) have been further researched[6-8]. Up to now, InAsSb epilayers have been prepared on many substrates such as GaAs, GaSb, InAs, InSb and InP by different methods such as molecular beam epitaxy (MBE)[9, 10], metalorganic chemical vapor diposition (MOCVD)[11, 12] and liquid phase epitaxy (LPE)[13, 14]. However, it is still a challenge to prepare high-quality InAsSb alloy due to lack of proper substrate. Comparing with InAs and GaSb substrates, GaAs substrate is more attractive for its cheap price and insulating property, although it has much larger lattice mismatch with InAsSb epilayers. Due to the large lattice mismatch(7.2%to14.6%)between the InAsSb epilayer and GaAs substrate, it is very difficult to prepare high-quality InAsSb epitaxial films, especially for the long-wavelength films. Middle As(Mid-As)composition of the InAsSb(long-wavelength)films show poor crystalline quality due to alloy disordering and difficultly in the growth of the alloy owing to miscibility gap in the region. So it is important study the growth of high quality InAsSb films with mid-As composition for long wavelength detector.

In this letter, InAsSb films with different As composition (10%-40%) were prepared on the GaAs (001)substrates by MBE and characterized by atomic field force microscopy(AFM), scanning electron microscopy(SEM), high-solution X-ray diffraction(HR-XRD), and Fourier transform

infrared (FTIR) transmittance measurements. The results indicate that the samples with low As compositions have high crystal quality with mirror-like surface. With the increase of the As compositions of the InAsSb films, obvious red shift of absorption peaks of the samples were found. Raman spectroscopy and Hall characterization were used to study the evolution of the optical quality and electrical properties of InAsSb films with different As components

2. Experiment

InAsSb films were prepared on GaAs (001) substrates with molecular beam epitaxy method (RIBER 32 R&D). Oxide layer on the GaAs substrate surface was desorbed first at about 600 °C with the As atmosphere, then a InSb buffer-layer was prepared with a two step growth method. The InAsSb films were prepared at different conditions, the accurate growth parameters were listed in the table 1. The growth rate of the InAsSb films is about 750nm / hour. All the samples were grown under the monitor of reflection high-energy electron diffraction (RHEED). The As composition of the InAsSb films were examined by high resolution XRD (Bruker (D8) x-ray diffractometer). The surface morphology was characterized by atomic force microscopy (AFM) (Digital Instruments Nano Scope III) operating in contact mode with a Si₃N₄ tip. The Raman scattering experiments were performed on micro-Raman system (Jobin-Yvon LabRam-Infinity) at room temperature, while 633 nm line of an He-Ne laser was used for excitation. The transport properties were performed in a perpendicular magnetic field of 1-1.4T using the dc four probe method in van der pauw geometry, the films were patterned into a square with the contacts on the four corners, and the indium was used as the Ohmic contacts of the samples.

Table 1. The detail growth parameter of the InAsSb films

Sample	Thickness of InSb buffer-layer	flux ratio of As/Sb	Growth temperature	As composition
Sample 1	250nm	1.1	360°C	7.2%
Sample 2	250nm	1.5	360°C	19.2%
Sample 3	750nm	2.5	360°C	39.4%

3. Results and Discussion

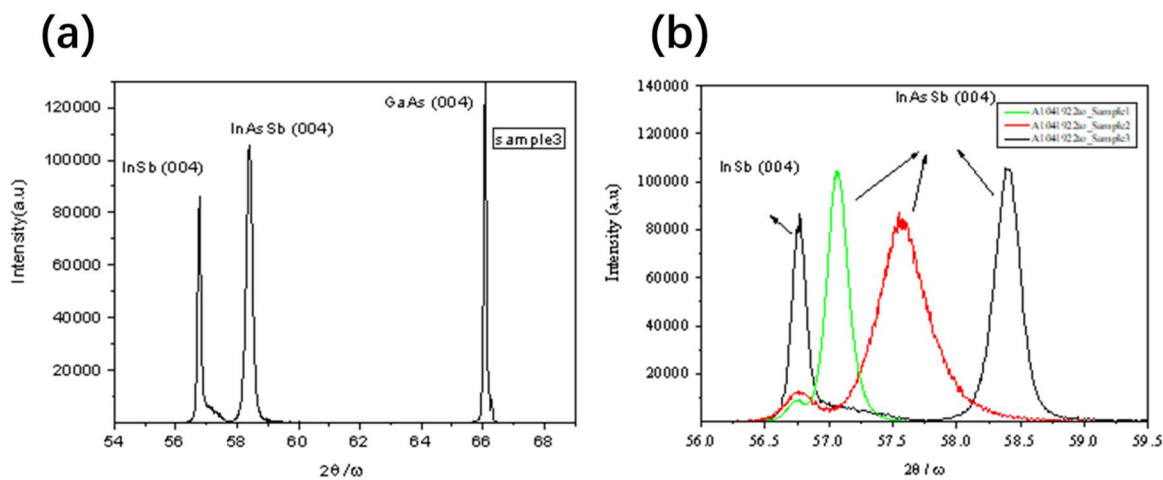


Fig. 1 The XRD (004) 2θ/ω curve of the samples: (a) the XRD (004) 2θ/ω curve of the sample 3 with all the peaks; (b) the XRD (004) 2θ/ω curve of the three samples with InSb and InAsSb peaks.

Fig. 1 shows the XRD (004) 2θ/ω curves of the InAsSb samples with different As composition. Fig. 1 (a) shows the XRD (004) 2θ/ω curve of the sample 3, in which the (004) peaks of the InSb, InAsSb

and GaAs are clearly observed. Fig.2 (b) shows the XRD (004) $2\theta/\omega$ curves of the three samples with different As composition, in which all the three InAsSb peaks and the peaks shift due to the distinction of the As composition are clearly observed. Due to the InSb buffer-layers of the sample 1 and sample 2 are much thinner than sample 3, the intensity of InSb peaks are relative weak. The As composition could be derived from the XRD results assuming the Vegard's law. The As composition of the three samples got from Fig.1 (b) are listed in the table 2. It can be seen that the As composition can be raised by increasing the As/Sb flux ratio. The XRD full-width at half maximum (FWHM) of the three samples are also listed in the table 2. The FWHM values of the samples are smaller than that of the InAsSb samples with same As composition have been reported[10]. From the XRD results, that the values of FWHM of the InAsSb films are increase with the increasing of the As composition, which means the crystal quality of the InAsSb films degenerate with the increasing of the As composition, the characterizations of the AFM and Raman spectra mentioned following also reveal similar result.

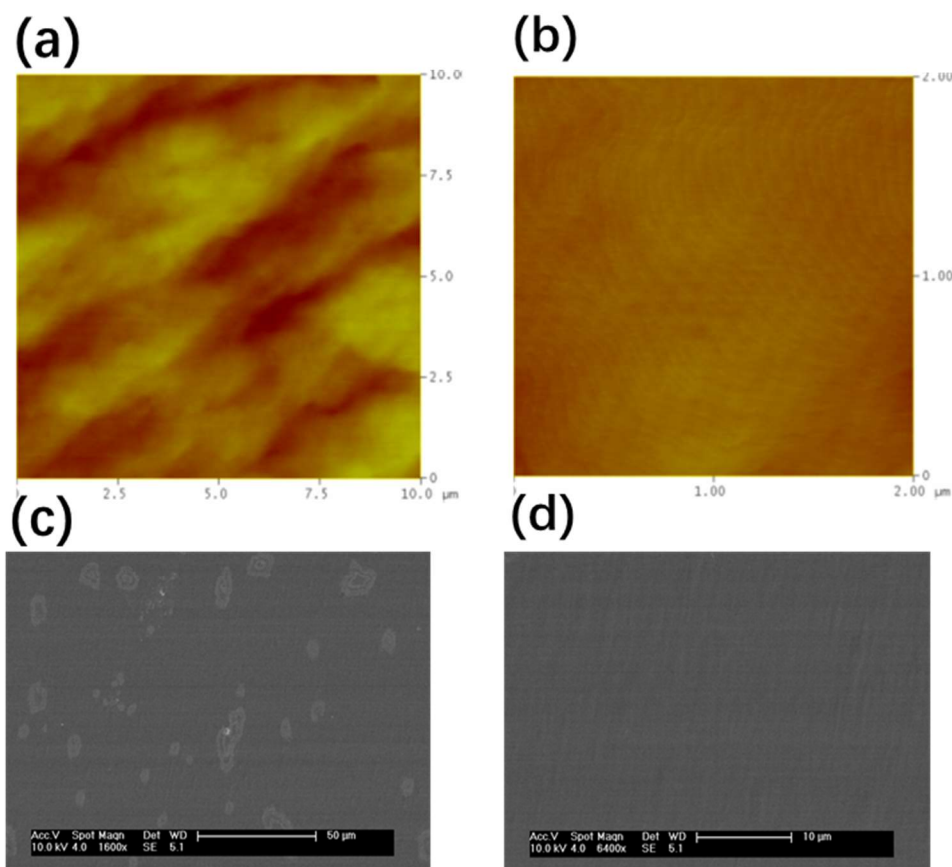


Fig. 2 surface morphology of sample 1 and sample 3: (a) the AFM image of sample 1 with image size of $10 \times 10 \mu\text{m}$; (b) the AFM image of sample 1 with image size of $2 \times 2 \mu\text{m}$; (c) the SEM image of sample 3 with a bar of $50 \mu\text{m}$; (d) the SEM image of sample 3 with a bar of $10 \mu\text{m}$.

Fig.2 shows the morphology of InAsSb sample1 and sample3. Fig.2 (a) shows the AFM image of sample 1 with the image size of $10 \times 10 \mu\text{m}$, the root mean square (RMS) value of which is 1.44 nm. Fig.2 (b) shows the AFM image of the sample 1 with the image size of $2 \times 2 \mu\text{m}$, from which it can be seen clearly the two-dimensional growth, the RMS value of which is only 0.44 nm. Both the Fig.2 (a) and Fig.2 (b) indicate that the sample 1 has a very smooth surface. Fig.2 (c) shows the SEM image of the sample 3, from which some spots with different shape and size can be observed, the physical mechanism of the growth are not clear. Fig.2 (d) shows the SEM image of the sample 3 with a bar of $10 \mu\text{m}$, although the surface of the sample is not very flat, while no island-like structure was observed.

Table 2. The electronic properties of the InAsSb films.

Sample	Temperature (K)	Mobility (cm ² /vs)	Concentration (cm ⁻³)
Sample 1	300	13100	1.02×10 ¹⁷
Sample 3	300	4812	1.73×10 ¹⁷
InSb film	300	39450	2.14×10 ¹⁷

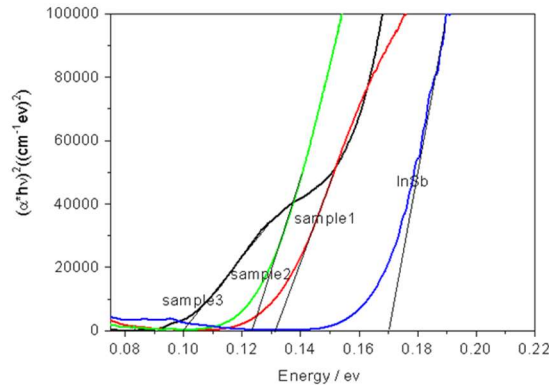


Fig. 3 Absorption spectra at room temperature for the three InAsSb samples and InSb reference sample.

Absorption spectra of the InAsSb films at room temperature (RT) was determined from transmission measurement using a FTIR spectrometer. Fig.3 shows the RT photon energy dependence of the $(\alpha \cdot hv)^2$, in which the sharp absorption edges of sample 1, sample 2 and InSb reference were observed, the special linearity of sample 3 should attribute to the contribution thicker InSb buffer-layer. Due to direct allowed optical transitions between parabolic bands should appear as straight lines, experimental absorption edges typically fit the expression $(h\nu\alpha)^2 = A(h\nu - E_g)$ [15], the fundamental band-gap (E_g) can be estimated from the intercept, as shown in the Fig.3. From Fig.3 it can be seen that the band gap of InAsSb reduce obviously compared to InSb reference sample, and the band gap reduce with the increasing of the As composition. The band gap of sample 3 achieves 0.10 eV at room temperature.

The results of the Hall measurement of the InAsSb films are shown in the table 2. Both sample 1 and sample 3 show the high mobility at room temperature. However, it can be seen that the electrical quality of the InAsSb films degenerate dramatically compare to the InSb film with the similar growth condition. The mobility of the InAsSb films decrease obviously with the increasing of the As composition, and simultaneously the carrier concentration increase quickly. The reason for degenerate of the electrical property is the plentiful dislocation come from the larger lattice mismatch between the eptiaxial film and the GaAs substrate. Although the density of the dislocation decrease dramatically with the increase of the distance to the interface, the influence of the dislocation scattering can not be neglect for thin films. Large alloy disorder also leads to lattice scattering of InAsSb films, and cause the decrease of mobility. At same time, we find the mobility of the mid-As composition InAsSb film at 77K (about 1422cm²/vs) is quite lower compared with that of room temperature. Generally, four scattering mechanisms (the ionized impurity scattering, piezoelectric potential scattering, deformation potential scattering and polar optical scattering) are used in III-V semiconductor materials to characterize the migration characteristics. Usually, the ionized impurity scattering is dominated in low temperature. In the mid- As composition InAsSb film, there is higher concentrations of impurities compare with the other samples. Due to the impurity scattering, the mobility of the material decreased significantly at low temperatures.

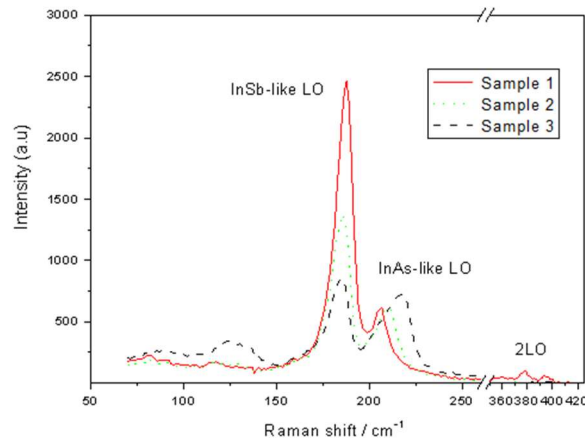


Fig. 4 The room temperature Raman spectra of the sample 1, sample 2, sample 3.

Fig.4 shows the room temperature Raman spectra of the sample 1, sample 2 and sample 3. As the previous report[16], both first order InAs-like and InSb-like LO peaks are observed in the Raman spectra of the three InAsSb films with different As composition. From the figure it also can be seen clearly that the red shift (toward lower wave number) of the InSb-like LO peaks and blue shift (toward lower wave number) linearly of the InAs-like LO peaks with the increasing of the As composition. The intensity of InSb-like LO peaks decrease with the increasing of the As composition and the InAs-like LO peaks increase simultaneously. Second order LO peaks at 378 cm-1 and 395 cm-1 in the Raman spectra of sample 1 are observed, which indicate that sample 1 has better crystal quality than the sample 2 and sample 3. A weak peak at 125 cm-1 belongs to sample 3 is found, indicating the crystal quality of the InAsSb films degenerate with the increase of the As composition. Recently, two additional peaks (round 44 cm-1 and round 130 cm-1) were observed in the Raman spectra of InAsSb appear[17], while they are not existing neither in pure InAs nor in InSb. Energies of 44 cm-1 and 130 cm-1 are close to phonon energy for momentum equals K and L for InAs. This type of peaks are usually called Disorder Activated Longitudinal Acoustic phonons (DALA) and Disorder Activated Transverse Acoustic phonons (DATA) and it is commonly accepted that they come from disorder in crystal field. The peak at 125 cm-1 ,which similar with the DATA peak reported, might come from the disorder of the InAsSb with high As composition.

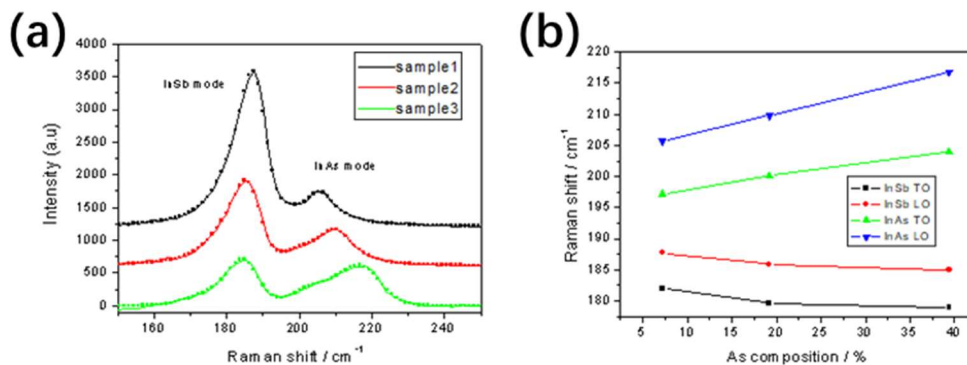


Fig. 5 (a) The room-temperature Raman spectra of three InAsSb/GaAs film samples with different compositions, with the solid line being the experimental data and the dots being the fitting data. (b) The relationship between the phonon modes of InSb and InAs and the As components obtained by fitting the experimental data.

In order to study the relationship between the phonon mode and the As component of InAsSb films, Raman spectra are well fitted as shown in Fig. 5(a). The detailed results of the fitting are shown in Fig. 5(b). It can be clearly seen that the two-mode behavior of the InAsSb films. The frequency of the InSb mode and InAs mode move in opposite directions as the As component increase. The InAs-like LO peak intensity increases with an increase in As composition and a blue shift was observed in the phonon peak frequency. The peak positions of InAs-like LO phonons can be fitted by linear least-squares method. In addition to LO phonon peak, both InSb and InAs-like TO phonon modes were observed as a weak peak although they are forbidden from (100) surface may be due to the slight sample misalignment. From Fig. 5(b), with the change of As components of InAsSb films, the evolution of TO mode is consistent with LO phonon mode.

4. Conclusion

In summary, InAsSb films with different compositions have been prepared on GaAs (001) substrates. The FTIR transmission measurement revealed that the absorption edge of the sample with As composition 40% achieve 0.1eV The absorption edge obviously red shift was observed with the increasing of As composition. Both InAs-like and InSb-like LO peaks are observed in the Raman spectra of the InAsSb films. The two-mode behavior of the InAs_xSb_{1-x} films are also observed. The evolution of the crystal quality and electrical properties of InAsSb films with different As components were studied in detail.

References

- [1] H. Shao, W. Li, A. Torfi, D. Moscicka, and W. I. Wang, Room-temperature InAsSb photovoltaic detectors for mid-infrared applications[J]. IEEE Photon. Technol. Lett.,18, (2006) 175. DOI:10.1109/LPT. 2006. 879941.
- [2] J. D. Kim, D. Wu, J. Wojkowski, J. Piotrowski, J. Xu, M. Razeghi, Long-wavelength InAsSb photoconductors operated at near room temperatures (200–300 K)[J]. Appl Phys Lett 68 (1995)1. DOI:10.1063/1.116784.
- [3] B. Bansal, V. K Dixit, V. Venkataraman, H. L. Bhat, Temperature dependence of the energy gap and free carrier absorption in bulk InAs_{0.05}Sb_{0.95} single crystals[J]. Appl Phys Lett 82 (2003) 26. DOI:10.1063/1.1587002.
- [4] C.T. Peng, N.F. Chen, F.B. Gao, X.W. Zhang, C.L. Chen, J.L. Wu, Y.D. Yu, Yude Yu, Liquid-phase-epitaxy-grown InAs_xSb_{1-x}/GaAs for room- temperature 8–12 μm infrared detectors[J]. Appl Phys Lett. 88 (2006) 242108. DOI:10.1063/1.2209709.
- [5] Y. Sharabani, Y. Paltiel, A. Sher, A. Raizman, A. Zussman. InAsSb/GaSb heterostructure based mid-wavelength-infrared detector for high temperature operation[J]. Appl Phys Lett. 90 (2007) 232106. DOI: 10.1063/1.2746951.
- [6] J.C.Tong, L.Y.MTobing, S.P.Qiu, D.H.Zhang, A.G.UPerera.Room temperature plasmon-enhanced InAs_{0.91}Sb_{0.09}-based heterojunction n-i-p mid-wave infrared photodetector [J]. Appl Phys Lett. 113 (2018) 011110. DOI: 10.1063/1.5018012.
- [7] C.Y.Jia , G.R. Deng , L.N. Liu, P. Zhao, G.F. Song, J.G.Liu and Y.Y.Zhang .Antimonide-based high operating temperature infrared photodetectors and focal plane arrays: a review and outlook[J]. Appl. Phys. 56 (2023) 433001. DOI:10.1088/1361-6463/acdefa.
- [8] H. Zhong, C. Lia, D.Q. Guo, K.M.Cheng, X.Y Tang. High performance InAs_{0.91}Sb_{0.09} MWIR detectors with an AlAs_{1-y}Sb_y graded barrier[J]. Infr Phys Technol.130(2023)104584 DOI:10.1016/j.infrared. 2023.104584.
- [9] S.Nakamura, P.Jayavel, T.Koyama, Y.Hayakawa. Investigations on the effect of InSb and InAsSb step-graded buffer layers in InAs_{0.5}Sb_{0.5} epilayers grown on GaAs (001)[J]. Crystal Growth 300,(2007), 497 DOI:10.1016/j.jcrysgr.2006.11.298.
- [10]H.C. Gao, W.X. Wang, Z.W. Jiang, L.S. Liu, J.M. Zhou, H. Chen. The growth parameter influence on the crystal quality of InAsSb grown on GaAs by molecular beam epitaxy[J]. Crystal Growth 406, (2007) 308 Doi:10.1016/j.jcrysgr.2007.08.018.

- [11] Tingting Wang, Min Xiong, Yingchun Zhao, Xu Dong, Yu Zhao, Jingjun Miao, Yong Huang⁴, Baoshun Zhang, Lixin Cao and Bohua Dong. Planar mid-infrared InAsSb photodetector grown on GaAs substrates by MOCVD[J]. Appl Phys Express 1212,2009. DOI:10.7567/1882-0786/ab507c.
- [12] R. M. Biefeld, S. R. Kurtz and A. A. Allerman The metal-organic chemical vapor deposition growth and properties of InAsSb mid-infrared (3-6- μm) lasers and LEDs, in IEEE Journal of Selected Topics in Quantum Electronics, 3, (1997) 739doi: 10.1109/2944.640629.
- [13] J. L. Zyskind, A. K. Srivastava, J. C. De Winter, M. A. Pollack, J. W. Sulhoff, Liquid-phase-epitaxial InAs_{1-y}Sb_y on GaSb substrates using GaInAsSb buffer layers: Growth, characterization, and application to mid-IR photodiodes [J].Appl. Phys. 61 (1987) 2898. <https://doi.org/10.1063/1.337834>.
- [14] S. H. Hu, C. H. Sun, Y. Sun, J. Ge, R. Wang, J. Wu, Q. W. Wang, N. Dai. High quality of InAsSb epilayer with cutoff wavelength longer than 10 μm grown on GaAs by the modified LPE technique[J]. Crystal Growth 2309-2312 (2009) 311. <https://doi.org/10.1016/j.jcrysgro.2009.02.037>.
- [15] J. Callaway (Ed.). Quantum Theory of the Solid State, Academic Press, New York, 1974 p.525.
- [16] Y. B. Li, S. S. Dosanjh, I. T. Ferguson, A. G. Normant, A. G. de. Oliveira, R. A. Stradling, R. Zallen, Raman scattering in InAs_{1-x}Sb_x alloys grown on GaAs by molecular beam epitaxy Semicond[J]. Sci Technol. 567-570 (1992) 7. DOI 10.1088/0268-1242/7/4/022.
- [17] K. Grodecki, K. Murawski, K. Michalczewski, B. Budner, and P. Martyniuk Raman scattering of InAsSb [J]. AIP Advances 9, 025107 (2019); <https://doi.org/10.1063/1.5081775>.